Investigation of an a-Si/c-Si interface on a c-Si(P) substrate by simulation*

Wang Jianqiang(汪建强)[1,†], Gao Hua(高华)[1], Zhang Jian(张剑)[1], Meng Fanying(孟凡英)[2], and Ye Qinghao(叶庆好)[3]

[1]Shanghai ChaoRi Solar Energy Science & Technology Co., Ltd, Shanghai 201406, China
[2]Shanghai Institute of Microsystem and Information Technology, Chinese Academy of Sciences, Shanghai 200050, China
[3]Department of Physics, Shanghai Jiao Tong University, Shanghai 200240, China

Abstract: We investigate the recombination mechanism in an a-Si/c-Si interface, and analyze the key factors that influence the interface passivation quality, such as Q_s, δ_p/δ_n and D_{it}. The polarity of the dielectric film is very important to the illustration level dependent passivation quality; when $n\delta_n = p\delta_p$ and the defect level E_t equal to E_i (c-Si), the defect states are the most effective recombination center, AFORS-HET simulation and analysis indicate that emitter doping and a-Si/c-Si band offset modulation are effective in depleting or accumulating one charged carrier. Interface states (D_{it}) severely deteriorate V_{oc} compared with J_{sc} for a-Si/c-Si HJ cell performance when D_{it} is over 1×10^{10} cm^{-2}·eV^{-1}. For a c-Si(P)/a-Si(P$^+$) structure, ϕ_{BSF} in c-Si and ϕ_0 in a-Si have different performances in optimization contact resistance and c-Si(P)/a-Si(P$^+$) interface recombination.

Key words: a-Si/c-Si interface; a-Si emitter property; interface defect states
DOI: 10.1088/1674-4926/33/3/033001 **EEACC:** 2500

1. Introduction

An a-Si/c-Si hetero-junction (HJ) solar cell has attracted a good deal of attention due to its unique high V_{oc} and its high efficiency a-Si/c-Si cell[1]. Compared with a traditional homo-junction cell, the most obvious advantages of an a-Si/c-Si cell are its tunable band offset, an a-Si low deposition temperature (< 200 ℃) and better cell temperature coefficient (–0.25%)[2, 3]. It is well known that a device quality a-Si emitter and an excellent interface quality between a-Si/c-Si are the key factors for a high efficiency HJ cell. The property of an a-Si emitter is still disputed, such as the band offset between the a-Si/c-Si band structure[4]. Defect states at the a-Si/c-Si interface cause a strong interface recombination in an HJ cell, when the interface defect density is more than 1×10^{13} cm^{-2}·eV^{-1}, a low interface state of 5×10^{11} cm^{-2}·eV^{-1} in the mid-gap could be achieved by wet-chemical smoothing and subsequent HF treatment. The detrimental effects of an epitaxially grown interface usually cause a V_{oc} of an a-Si/c-Si cell of less than 600 mV. The energy position within the band gap and capture cross section of the electron and hole determine the defects in the epitaxial film, usually abruptness of the a-Si/c-Si interface without initial epitaxial growth is preferred[5]. To date, the highest confirmed efficiency in an experiment on a c-Si (P-type) substrate is 18.4%. For an a-Si/c-Si HJ cell investigation, the above mentioned issues should be carefully considered.

In this paper, a p-type c-Si based a-Si/c-Si HJ cell has been developed to analyze the influence of an a-Si emitter and a-Si/c-Si interface states on HJ cell efficiency. Experimentally controllable methods are considered in this work. As a result, a simulated cell efficiency of 22.27% with optimized parameters on a p-type c-Si substrate is given.

2. AFORS-HET simulation model

AFORS-HET[6], a one-dimensional device simulation software developed at Helmholtz Zentrum Berlin (HZB), is used to investigate a TCO/a-Si(N$^+$)/c-Si(P)/Al-BSF(P$^+$) HJ cell. It solves the Poisson equation and two carrier continuity equations by finite difference and Newton–Raphson techniques, under a non-equilibrium steady state condition.

In this model cell, an 80 nm front TCO layer and 5 μm aluminum layer BSF(P$^+$) both forming a flat band with an a-Si(N$^+$) and c-Si(P) substrate respectively are assumed. For N-type and intrinsic a-Si:H materials, the density of localized states in the mobility gap have been set using the generally accepted density of states (DOS). Donor-like states (D$^{+/0}$ in the lower half of the band gap) and accepter-like states (D$^{0/-}$ in the upper half of the band gap) consist of exponential distribution band tail states and Gaussian distributions of dangling bonds[7, 8]. Figure 1 is the band structure of a TCO/a-Si(N$^+$)/a-Si(i)/c-Si(P)/Al-BSF(P$^+$) HJ cell. Parameters that influence HJ cell efficiency are depicted in Fig. 1, such as interface defect density (D_{it}), the band offset between a-Si and c-Si (ΔE_c and ΔE_v), the bias voltage in the a-Si ($V_{b(a\text{-}Si)}$) and c-Si ($V_{b(c\text{-}Si)}$) side. All the main parameters used in AFORS-HET simulation are listed in Table 1, which include the basic material quality of a-Si and c-Si, the a-Si/c-Si interface property, and the bandtail distribution model in a-Si layers.

AFORTH-HET requires a single-electron scheme to model carrier recombination in a-Si bulk and at the a-Si:H/c-Si interface. Dangling bonds are therefore described by two recombination levels located at $E_{+/0}/E_{0/-}$.

* Project supported by the International Joint Foundation of Shanghai Science & Technology Commission with Applied Material, China (No. 08520741400) and the Talent Foundation of Shanghai Science & Technology Commission, China (No. 08XD14022).
† Corresponding author. Email: wangwjq@gmail.com
Received 23 June 2011

Table 1. Main parameters for a TCO/a-Si(N^+)/c-Si(P)/Al-BSF(P^+) cell.

General parameter	a-Si(N^+)/a-Si(i)/c-Si(P)	
Thickness (cm)	$3\times10^{-7}/4\times10^{-7}/3\times10^{-2}$	
Electron affinity, χ (eV)	3.9/3.9/4.05	
Band gap, E_g (eV)	1.74/1.74/1.12	
Effective E_c density, N_c (cm^{-3})	$1\times10^{20}/1\times10^{20}/2.8\times10^{19}$	
Effective E_v density, N_v (cm^{-3})	$1\times10^{20}/1\times10^{20}/1.04\times10^{19}$	
Electron mobility, μ_n ($cm^2/(V\cdot s)$)	5/5/1041.1	
Hole mobility, μ_p ($cm^2/(V\cdot s)$)	1/1/412.9	
Donor doping density, N_D (cm^{-3})	$1\times10^{20}/0/0$	
Acceptor doping density, N_A (cm^{-3})	$0/0/1.5\times10^{16}$ ($\sim$1 $\Omega\cdot$cm)	
Defects	c-Si(P)	
Density of states ($cm^{-3}\cdot eV^{-1}$)	1×10^{11} @ 0.55 eV above E_V	
Band tail state exponential distribution	a-Si(N^+)	a-Si(i)
N_{BV}/N_{BC} at band edge ($cm^{-3}\cdot eV^{-1}$)	$2\times10^{21}/2\times10^{21}$	$1\times10^{21}/1\times10^{21}$
Urbach energies $E_{tail,V}$ and $E_{tail,C}$ (eV)	0.106/0.068	0.045/0.03
Dangling bond state Gaussian distribution	a-Si(N^+)	a-Si(i)
$E_{+/0}/E_{0/-}$ (eV)	0.46/0.66	0.8/1
S_{DB} (eV)	0.22	0.15
Density of dangling bonds ($cm^{-3}\cdot eV^{-1}$)	1.78×10^{20}	1.49×10^{17}
Interface defect density (D_{it})	a-Si/c-Si	
Density of defects ($cm^{-2}\cdot eV^{-1}$)	1.2×10^{11} (Continuous)	

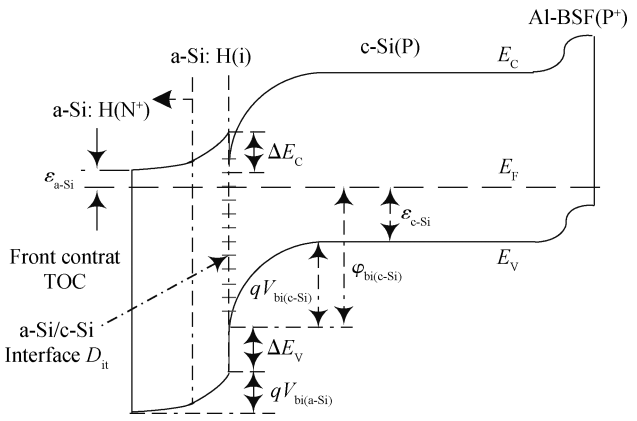

Fig. 1. Band structure of a TCO/a-Si(N^+)/a-Si(i)/c-Si(P)/Al-BSF(P^+) HJ cell.

$$N_{+/0}(E)=\frac{N_{DB}}{S_{DB}\sqrt{2\pi}}\exp\left[-\frac{1}{2}\left(\frac{E_{+/0}-E}{S_{DB}}\right)^2\right], \quad (1)$$

$$N_{0/-}(E)=\frac{N_{DB}}{S_{DB}\sqrt{2\pi}}\exp\left[-\frac{1}{2}\left(\frac{E_{0/-}-E}{S_{DB}}\right)^2\right], \quad (2)$$

where $E_{+/0}=E_{center}-kT\ln 2$ and $E_{0/-}=E_{center}+U_{eff}+kT\ln 2$, the distance between energy levels $E_{+/0}$ and $E_{+/-}$ is the correlation energy $U_{eff}=E_{0/-}-E_{+/0}$ of the dangling bond defects. It depends on the Coulomb interaction of the electrons within the dangling bonds, and on contributions due to the lattice relaxation, electron–phonon interactions and re-hybridization of the dangling bond orbital.

The interface between a-Si(N^+)/c-Si(P) is described by inserting a thin (about 1 nm) defective c-Si layer (with a band gap of 1.12 eV) between bulk c-Si and the a-Si:H layer. The defect distribution in the a-Si(N^+)/c-Si(P) interface layer is taken as constant through its band gap, assuming donor/acceptor-like defects in the lower/upper part of the defective c-Si band gap. The interface defect density (D_{it}) varies between 10^9 and 10^{15} $cm^{-2}\cdot eV^{-1}$, the electron and hole capture cross sections are fixed at 10^{-14} cm^2, the other main parameters are fixed according to the default values in the software.

3. Recombination at the a-Si/c-Si interface

Recombination through defects levels in a semiconductor is usually described by Shockley–Read–Hall theory[9, 10]. A single trap level recombination rate R_{SRH} [$cm^{-3}\cdot s^{-1}$] given by SRH theory is given by[11]

$$R_{SRH}(n,p)=\frac{np-n_i^2}{\dfrac{n+n_ie^{(E_t-E_i)/KT}}{\delta_p}+\dfrac{p+n_ie^{-(E_t-E_i)/KT}}{\delta_n}}\times\nu_{th}N_t. \quad (3)$$

where N_t (cm^{-3}) is the defect density, δ_p (cm^2) and δ_n (cm^2) are the capture cross-section of holes and electrons, $\nu_{th}\approx 2\times10^7$ cm/s is thermal velocity of the charged carriers, when $n\delta_n=p\delta_p$ and the defect level E_t equal to E_i, $R_{SRH}(n,p)$ will approach its maximum value. SRH recombination limits the lifetime of silicon bulk mainly at a low injection level ($10\,n_i<\Delta n<10\,N_{dop}$), N_{dop} is the doping density of the silicon wafer, and n_i is the intrinsic carrier density. Recombination through non-interacting surface states could be obtained by extending the SRH mechanism by integrating over all energy levels within the band gap.

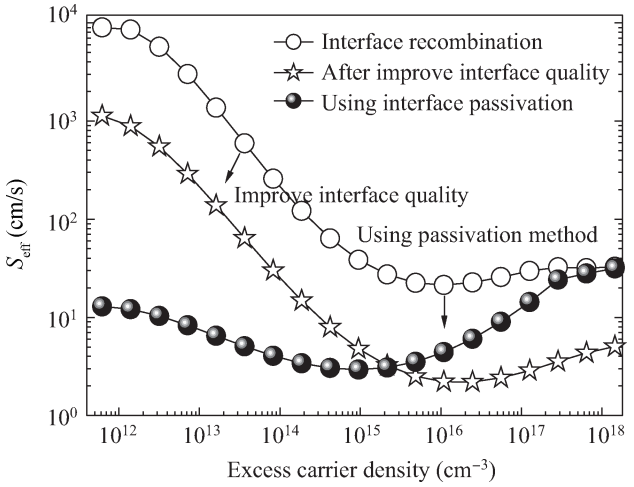

Fig. 2. Influence of surface field effect and interface defect states (D_{it}) on interface recombination.

$$U_{it}(n_s, p_s) = (n_s p_s - n_i^2)\upsilon_{th} \times \int_{E_V}^{E_C} D_{it}(E_t) \left\{ \frac{n_s + n_i \exp[(E_t - E_i)/kT]}{\delta_p} + \frac{p_s + n_i \exp[-(E_t - E_i)/kT]}{\delta_n} \right\}^{-1} dE_t. \quad (4)$$

According to Eq. (4), there are two possible ways to improve the a-Si/c-Si surface passivation quality. From the simulation in Fig. 2, we can see that at low carrier injection levels, the surface filed is much more effective at improving interface recombination. At high carrier injection levels, the surface filed effect is gradually eliminated, and improving the interface status is preferred to achieve a high quality interface.

(1) Reduction of D_{it}: Through chemically saturating dangling bonds with hydrogen or oxygen atoms, this could be resolved by passivation of the surface by dielectric layers such as SiO_2, SiN_x and a-Si:H. Deep level states near the mid-gap are the most effective recombination centers, eliminating deep surface energy levels is the focus of improving a-Si/c-Si interface states. (2) Reduction of carrier density (n_s or p_s): The field-effect is an effective way to deplete one carrier and accumulate another charged carrier at the a-Si/c-Si interface.

Interface recombination velocity of a double sided symmetrically passivated c-Si substrate can be expressed as follows:

$$S_{eff} = \left(\frac{1}{\tau_{eff}} - \frac{1}{\tau_{bulk}} \right) \frac{W}{2}, \quad (5)$$

where τ_{bulk} is the lifetime of the silicon substrate, and it can be given by $\frac{1}{\tau_{bulk}} = \frac{1}{\tau_{extr}} + \frac{1}{\tau_{intr}}$, τ_{extr} is the effective lifetime correlated with defect recombination, τ_{intr} is the intrinsic lifetime of silicon substrate related to Auger/radiative recombination.

When considering a-Si/c-Si interface recombination, the effective lifetime of a-Si/c-Si structure can be as follows[12]:

$$\tau_{eff}^{-1} = \tau_{bulk}^{-1} + \frac{2}{W} \frac{1}{\Delta n} U_{it}(\Delta n; n_0, p_0; Q_s, D_{it}; \delta_p, \delta_n). \quad (6)$$

From Eq. (6), we can see that the interface recombination of the a-Si/c-Si structure is mainly determined by Δn, δ_p/δ_n, Q_s and D_{it}.

We know that the carrier density of the electron and hole at the a-Si/c-Si structure interface is determined by surface potential and can be expressed by:

$$n_s = (n_0 + \Delta n) \exp(q\phi_s/kT), \quad (7)$$

$$n_s = (p_0 + \Delta p) \exp(-q\phi_s/kT), \quad (8)$$

the charge in c-Si surface is given by[13]:

$$Q_s = \mathrm{sign}(\varphi_s) \times \left\{ \frac{2kTn_i\varepsilon_0\varepsilon_{si}}{q^2} \left[e^{q(\phi_p - \varphi_s)/kT} - e^{q\phi_p/kT} + e^{q(\varphi_s - \phi_n)/kT} - e^{-q\phi_n/kT} + \frac{q\varphi_s(p_0 - n_0)}{kTn_i} \right] \right\}^{1/2}, \quad (9)$$

where ϕ_p and ϕ_n are the quasi-Fermi level of hole and electron at the edge of space charge region, and φ_s can be calculated from the expression of Q_s.

In order to avoid the injection level dependent additional bulk recombination losses in the inversion layer close to the c-Si surface[14, 15] a different type of doping emitter has properly passivated dielectric thin films. A highly doped p-type c-Si surface should be passivated by a negatively charged thin film such as Al_2O_3, and the positively charged dielectric film, i.e., thermal SiO_2, a-SiC:H and a-SiN_x:H lead to a high level of surface passivation on lightly doped n- and p-type c-Si and a highly doped n-type c-Si surface[16]. The passivation of the a-Si/c-Si structure could be modulated through redistributing the different charge status of the rechargeable defects.

4. Influence of an emitter property on a-Si/c-Si interface passivation

4.1. Influence of a-Si(N^+)/c-Si band offset

According to Anderson's law[17], diffusion potential (V_{bi}) across an a-Si(N^+)/c-Si(P) HJ structure in Fig. 1 can be expressed as follows:

$$qV_{bi} = qV_{bi(a\text{-}Si)} + qV_{bi(c\text{-}Si)} = E_{g(c\text{-}Si)} - \xi_{(a\text{-}Si)} - \xi_{(c\text{-}Si)} + \Delta E_c, \quad (10)$$

where $V_{bi(a\text{-}Si)}$ and $V_{bi(c\text{-}Si)}$ are the diffusion potential in a-Si and c-Si(P), $\xi_{(a\text{-}Si)}$ and $\xi_{(c\text{-}Si)}$ are the distances between the Fermi level and the nearest band for a-Si and c-Si respectively. Conduction and valence band offset in an a-Si/c-Si HJ structure could be determined by the difference of electron affinity (χ) between a-Si and c-Si layers. We can see that a high minority carrier band gap offset (ΔE_C) is attributed to high V_{oc} in an a-Si(N^+)/c-Si(P) HJ cell.

Figure 3 indicates the influence of the conduction band offset (ΔE_C) on TCO/a-Si(N^+)/c-Si(P)/Al-BSF(P^+) HJ cell performance, and the decreasing electron affinity (χ) of emitter a-Si(N^+) causes higher band bending in the c-Si(P) side, which is labeled as $qV_{bi(c\text{-}Si)}$. In simulating the influence of band offset on the performance of the a-Si(N^+)/c-Si(P) cell, we vary the

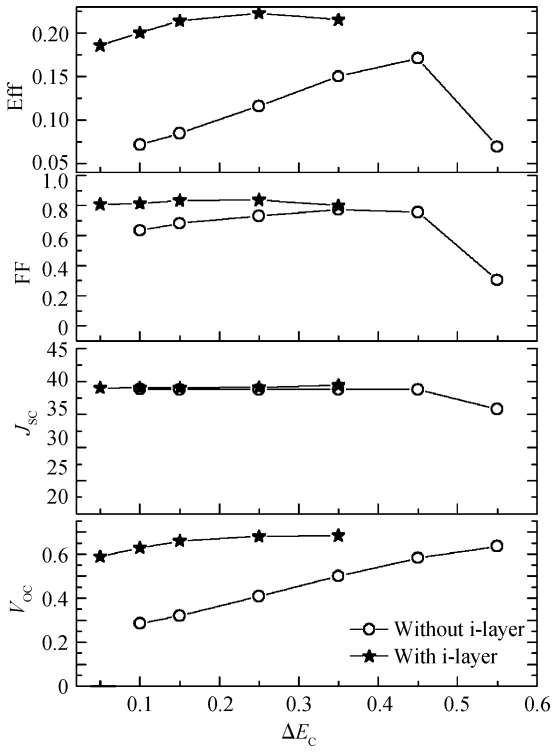

Fig. 3. Influence of the a-Si band offset (ΔE_C) on the a-Si (N^+)/a-Si(i)/c-Si(P)/Al-BSF(P^+) cell performance.

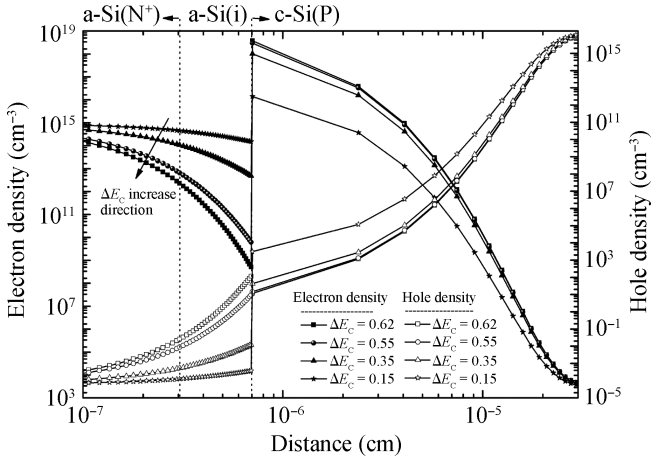

Fig. 4. Electron and hole density at the a-Si(i)/c-Si(P) interface at different conduct band offsets (ΔE_C).

electron affinity (χ) of a-Si(doped) and a-Si(intrinsic) simultaneously.

According to Eqs. (9) and (10), high $qV_{bi(c\text{-}Si)}$ (in Fig. 1) will enlarge the ratio of electron to hole (n_s/p_s) in a-Si(N^+)/c-Si(P). As the Shockley–Read–Hall (SRH) recombination process involves one hole and one electron, depleting one type of charge carrier is an effective way to reduce the interface recombination. Figure 4 shows the density of electron and hole at the a-Si(N^+)/c-Si(P) interface, an obvious inversion layer occurs on the c-Si side, and a big jump of electron density at the a-Si/c-Si interface in the reversion zone is observed. High conductance and low activation energy of the inversion layer on the c-Si side have been reported[18]. Higher ΔE_C at the a-Si/c-Si interface induces a larger value of carrier density ratio (n_s/p_s) and a wider inversion region on the c-Si(P) side. This could effectively reduce a-Si/c-Si interface recombination and enhance the interface conductance. A maximum value of 103 nm inversion layer on the c-Si(P) side is calculated when ΔE_C is equal to 0.62 eV.

The clear dependence of band offsets in a-Si/c-Si on the hydrogen content of an a-Si:H emitter layer has been reported: Van de Walle *et al.*[19] proposed that every one percent increase of hydrogen content in the a-Si layer will correspond to a 0.04 eV decrease of E_v for a-Si in a-Si/c-Si band structure. A wide range of experimental values for ΔE_V and ΔE_C in the a-Si/c-Si HJ structure have been reported: (1) ΔE_V varies from $\approx$ 0 eV[20] to 0.71 eV[21]; (2) ΔE_C varies from 0.09 V[21] to 0.6 eV[20]. The fluctuation of hydrogen distribution in a-Si:H material could lead to the perturbation of the band offset in an a-Si(N^+)/c-Si(P) structure[22].

With Eq. (12), we can see that for a P- or N-type silicon substrate HJ cell, the higher the minority carrier band offset (ΔE), the higher the V_{oc} of the a-Si/c-Si HJ structure cell. In this work, we mainly simulate the influence of ΔE_C on the a-Si(N^+)/c-Si(P) HJ cell. The modulation of hydrogen content in an a-Si film has provided an effective way to alter the band offset distribution in an a-Si/c-Si(P/N) structure.

Because the recombination probability in a heavily doped thin a-Si(N^+) emitter is close to unity[23], the optimizing a-Si(N^+) thickness is another issue we should consider during the thin layer deposition procedure. First the thickness of the a-Si(N^+) emitter should be larger than the sum of the depletion regions of the TCO/a-Si(N^+) and a-Si(N^+)/c-Si(P) structure on the a-Si(N^+) side, an overlap of these two depletion regions will cause the decrease of V_{oc} in the a-Si(N^+)/c-Si(P) structure[24]. Second, as the a-Si(N^+) emitter gets thinner, the density of this thin layer will alter the position of a-Si E_v in the a-Si/c-Si band structure. The relationship between the a-Si layer density variation and absolute potential deformation of a-Si E_v is given by[25]:

$$a_v = \mathrm{d}E_v/\mathrm{d}\ln\Omega, \quad a_v = 0.46\,\mathrm{eV}, \tag{11}$$

where $\mathrm{d}\ln\Omega = \mathrm{d}\Omega/\Omega$ is the fractional volume change under hydrostatic strain.

4.2. Influence of a-Si(N^+) emitter doping

For an a-Si(N^+)/c-Si(P) structure HJ cell, the band offset ΔE_c (about 0.15 eV) is a barrier to electron transport through the junction. The situation is especially severe for hole transportation in an a-Si(P^+)/c-Si(N) structure cell. Effective carrier transportation over a high barrier requires both a high space charge and a high a-Si:H density of state (DOS) to allow for the hopping process. A highly doped a-Si(N^+) emitter is indispensable to improve this situation.

Figure 5 indicates the influence of a-Si(N^+) emitter doping on the cell performance of an a-Si(N^+)/c-Si(P) HJ structure. Simulation results show that, under c-Si(P) substrate doping of 1.5×10^{16} cm^{-3} ($\sim$1 Ω·cm), a-Si(N^+) emitter doping of more than 1×10^{20} cm^{-3} is necessary to obtain high V_{oc} for a-Si(N^+)/a-Si(i)/c-Si(P) structure cell. After inserting a thin a-Si(i) layer, an obvious improvement in V_{oc} has been achieved, but there is not much variation in J_{sc}.

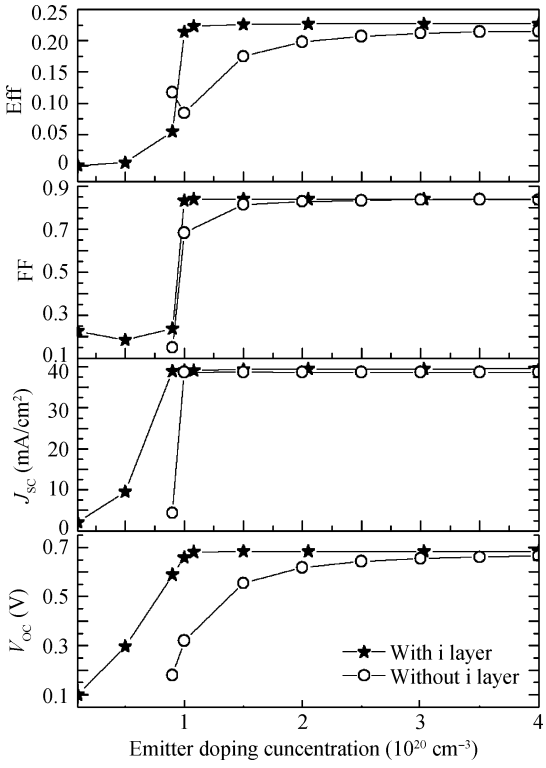

Fig. 5. Influence of emitter doping concentration on a TCO/a-Si(N^+)/a-Si(i)/c-Si(P)/Al-BSF(P^+) cell.

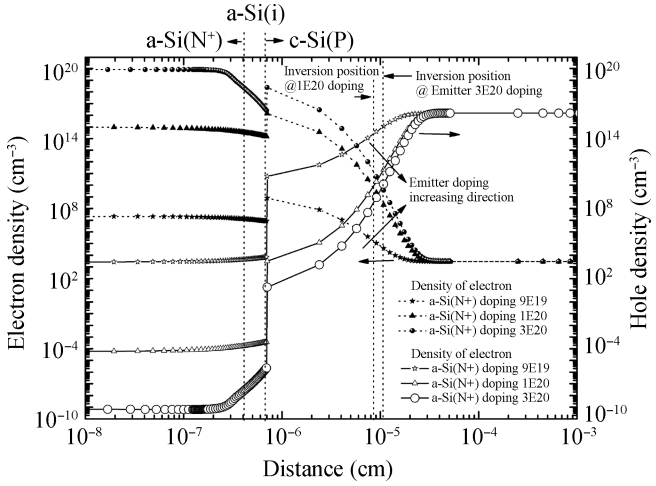

Fig. 6. Electron and hole density at an a-Si(i)/c-Si(P) interface at different emitter doping concentrations.

For an a-Si(N^+)/c-Si(P) structure cell with an a-Si(i) layer, an a-Si(N^+) doping concentration of more than 1×10^{20} cm^{-3} is necessary to obtain high V_{oc} and high efficiency of the a-Si(N^+)/c-Si(P) HJ solar cell, while the a-Si(N^+)/c-Si(P) structure cell without the a-Si(i) layer has to get a high emitter concentration to achieve high efficiency. Figure 6 depicts the density profile of electron and hole in an a-Si(N^+)/c-Si(P) structure at different emitter doping concentrations. When a-Si(N^+) doping is more than 1×10^{20} cm^{-3}, an obvious inversion region is also observed on the c-Si side like Fig. 4. The width of the inversion region and the value of the electron and hole ratio (n_s/p_s) both increase as a-Si(N^+) doping concentration gets higher.

In addition, highly doped emitter a-Si(N^+) will cause electron gas degeneration, which leads to a Burstein–Moss (B–M) band gap enlargement effect (ΔE_g^{B-M}) and a Many–Body band narrowing effect (ΔE_g^N)[26]. But, in this simulation we did not consider this effect on our simulation results.

$$E_g = E_g^0 + \Delta E_g = E_g^0 + \Delta E_g^{B-M} - \Delta E_g^N, \quad (12)$$

$$\Delta E_g^{B-M} = \hbar^2 (3\pi^2 n_e)^{2/3} / 2m_{cv}^*,$$

$$\Delta E_g^N = \hbar \Sigma_V(K_F, \omega) - \hbar \Sigma_C(K_F, \omega),$$

$$m_{cv}^* = \left(\frac{1}{m_c^*} + \frac{1}{m_v^*} \right)^{-1}, \qquad K_F = (3\pi^2 n_e)^{1/3}, \quad (13)$$

where E_g^0 is the band gap in the non-perturbation state, ΔE_g encompasses the Burstein–Moss shift, which is partially balanced by the Many–Body band gap narrowing effects. n_e and m_{cv}^* are the carrier density and effective mass respectively.

5. Influence of defect states (D_{it}) on a-Si(N^+)/c-Si(P) interface recombination

We know that the distribution of typical $D_{it}(E)$ at the a-Si/c-Si interface is a superposition of states near band edges and states symmetrically distributing about a minimum near mid-gap. These states are surface pretreatment induced strain bonds, dangling bonds, bonds between adsorbates, and silicon surface atoms of different oxidation leading to several groups of interface states. The minimum value of these rechargeable interface state distributions can be taken as a measure of the electronic quality of the wafer interface. A very low interface state density of about 1.2×10^{10} cm^{-2}·eV^{-1} could be obtained on an atomically flat H-terminated surface.

Figure 7 shows the dependence of V_{oc} and J_{sc} with a-Si(N^+)/c-Si(P) interface density states. Simulation results indicate that V_{oc} is much more sensitive to D_{it} compared with J_{sc}, when D_{it} at the a-Si(N^+)/c-Si(P) interface is over 1×10^{10} cm^{-2}·eV^{-1}. As D_{it} varies from 1×10^9 to 1×10^{15} cm^{-2}·eV^{-1}, a sharp decrease of V_{oc} from 0.68 to 0.25 V is observed, while J_{sc} remains constant initially and then starts to decay once D_{it} is over 1×10^{12} cm^{-2}·eV^{-1}.

When D_{it} in a-Si/c-Si is over 1×10^{13} cm^{-2}·eV^{-1}, recombination in a-Si/c-Si is strongly limited by D_{it}[8]. A higher D_{it} in an a-Si(N^+)/c-Si(P) interface will induce the localization of a space charge region on the c-Si(P) side, so the space charge region could not appreciably extend into the c-Si(P) absorber region. As a result, a high interface field and field collapse over an adjacent region of the c-Si(P) absorber layer will flatten the band bending on the c-Si(P) side, which could eventually cause a sharp decrease in V_{oc}; When D_{it} is less than 1×10^{10} cm^{-2}·eV^{-1}, a-Si/c-Si interface recombination is not the critical recombination channel because of a strong field at the a-Si(N^+)/c-Si(P) interface. Jensen[23, 27] reports that the major recombination of an a-Si/c-Si structure occurs in the neutral bulk of the c-Si side, and higher V_{oc} can only be obtained by improving the electronic quality of the c-Si substrate. So the quality of c-Si absorber, carrier lifetime and doping concentration, and back-surface recombination in the c-Si substrate play important roles in V_{oc} improvement. Photo-generated current

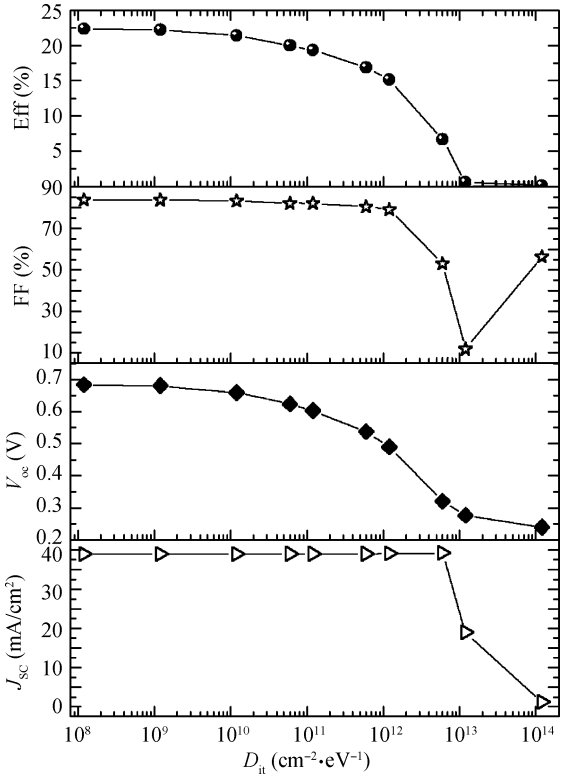

Fig. 7. Influence of interface states (D_{it}) on TCO/a-Si(N$^+$)/a-Si(i)/c-Si(P)/Al-BSF(P$^+$) cell performance.

is strongly determined by the recombination in the a-Si/c-Si interface and a-Si emitter.

In order to get a high quality interface in a-Si/c-Si, a-Si soft deposition methods such as hot-wire-CVD (HWCVD) and c-Si surface clean pretreatment are preferred. Besides improving the interface situation between an a-Si and c-Si heterojunction, the epitaxial growth interface on a c-Si substrate during a-Si:H deposition should also be avoided. This thin epitaxial growth layer usually causes a V_{oc} of an a-Si/c-Si cell of less than 600 mV, which has been reported many times[28, 29], a high defective epi-growth layer that extends through or forms a mixed phase with the a-Si(i) layer, which increases the interface density and deteriorates the junction interface quality. Abruptness of an a-Si/c-Si interface without initial epitaxial growth is usually preferred. The defects within the epitaxial growth layer are determined by their energetic position within the band gap and capture cross section of electron and hole[5]. H_2 pretreatment or inserting a thin a-Si(i) layer may provide an effective way to improve the HJ interface quality.

6. Optimization of a rear c-Si(P)/a-Si(P$^+$) structure

The effective rear surface passivation velocity depends on the density of minority carriers, and the series resistance of rear c-Si(P)/a-Si(P+) depends on the density of majority carriers. Figure 8 is the band diagram of the c-Si(P)/a-Si(P$^+$) structure. From Fig. 8 we can see that electrons have to overcome ϕ_{BSF} and ΔE_c to get to the c-Si(P)/a-Si(P$^+$) interface, meanwhile, holes should surpass and tunnel through the high ΔE_v to be collected.

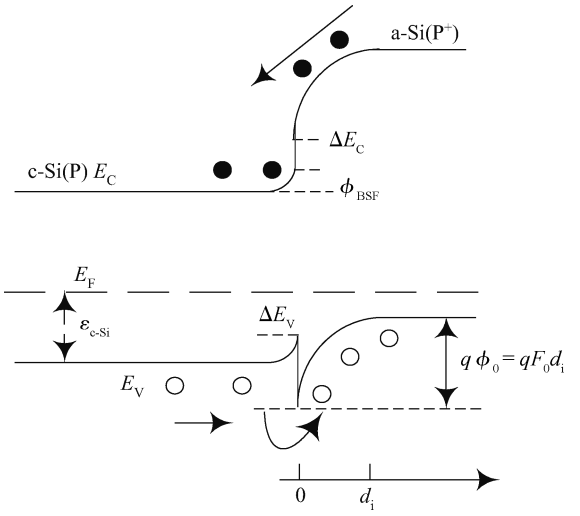

Fig. 8. Band diagram of a c-Si(P)/a-Si(P$^+$) structure.

According to the current continuity equation, the hole/electron current j_p and j_n can be expressed as follows:

$$j_p = q\frac{\phi_0 + V}{d_i}\mu_p p(0)\left[1 - \exp\left(-\frac{V}{V_{th}}\right)\right],$$

$$p(0) = N_A \exp\left(-\frac{\Delta E_V + q\phi_{BSF}}{kT}\right),$$

$$j_n(d_i) = n(0)\exp\left(\frac{-Fd_i}{V_{th}}\right)\frac{qF\mu_n}{F\mu_n + S_{ip}\left[1 - \exp\left(\frac{-Fd_i}{V_{th}}\right)\right]},$$

$$n(0) = n_b \exp\left(\frac{-\Delta E_C + q\phi_{BSF}}{kT}\right).$$

The contact resistance of the c-Si(P)/a-Si(P$^+$) structure is calculated as

$$R = \left(\frac{dj_p}{dv}\right)^{-1}\Bigg|_{V=0} = \frac{v_{th}d_i}{q\mu_p N_A\phi_0}\exp\frac{\Delta E_v - q\phi_{BSF}}{kT}.$$

The effective recombination velocity S_{eff} at a-Si(i)/c-Si(P) interface can be expressed as follows:

$$S_{eff} = S_{ip}\exp\frac{-(q\phi_0 + \Delta E_C + q\phi_{BSF})}{kT} \times\left\{1 + \frac{S_{ip}d_i}{\phi_0\mu_n}\left[1 - \exp\left(-\frac{q\phi_0}{kT}\right)\right]\right\}^{-1}. \quad (14)$$

When $S_{ip} \to \infty$, the peak value of S_{eff} can be expressed concisely as follows:

$$S_{eff,\,max} = \frac{\phi_0\mu_n}{d_i}\exp\frac{-(q\phi_0 + \Delta E_C + q\phi_{BSF})}{kT} \times\left[1 - \exp\left(-\frac{q\phi_0}{kT}\right)\right]. \quad (15)$$

According to the calculation, we can see that increasing the potential of ϕ_{BSF} in c-Si and ϕ_0 on the a-Si side are effective in

improving the contact resistance in the c-Si(P)/a-Si(P^+) structure. Compared with ϕ_0, a higher ϕ_{BSF} could more obviously decrease the contact resistance. A low enough contact resistance to avoid significant resistive loss in the c-Si(P)/a-Si(P^+) structure is only achieved for $\phi_{BSF} > 0.15$ eV. In respect of a-Si/c-Si(P) interface recombination, ϕ_0 has the much greater potential to acquire a high quality interface, the effective surface recombination is controlled by the sum of the potentials in the c-Si base and a-Si layer.

7. Conclusions

D_{it} and the ratio of n_s/p_s are the key factors for achieving a high passivation quality at the a-Si/c-Si interface. The polarity of the dielectric film is very important to the illustration level dependent passivation quality. AFORS-HET simulation and analysis indicate that a-Si/c-Si band offset modulation and a-Si emitter optimization could effectively increase the ratio of n_s/p_s. Emitter doping of over 1×10^{20} cm^{-3} is an indispensable condition in the a-Si(N^+)/c-Si(P) structure with an a-Si(i) thin layer to achieve high cell efficiency. For a TCO/a-Si(N^+)/a-Si(i)/c-Si(P)/Al-BSF(P^+) HJ cell, V_{oc} is much more sensitive to D_{it}, when comparing with J_{sc}. Obvious improvement in V_{oc} and cell efficiency is observed by inserting a thin a-Si(i) layer in the a-Si(N^+)/c-Si(P) HJ structure. ϕ_{BSF} in c-Si and ϕ_0 in a-Si have different performance in optimization contact resistance and c-Si(P)/a-Si(P^+) interface recombination. With optimized emitter doping and interface defect states, a cell efficiency of 22.27% is achieved with a V_{oc} of 680.2 mV.

Acknowledgements

Special thanks are given to Helmholtz Zentrum Berlin (HZB) for providing simulation software AFORS-HET.

References

[1] http://sanyo.com/news/2009/05/22-1.html (latest access date is 19.Oct.2010)
[2] Fuhs W, Niemann K, Stuke J. Heterojunctions of amorphous silicon and silicon single crystals. Proc 20th AIP Conference, 1974, 20: 345
[3] Taguchi M, Terakawa A, Maruyama E, et al. Obtaining a higher V_{oc} in HIT cells. Prog Photovoltaics, 2005, 13(6): 481
[4] Gudovskikh A S, Ibrahima S, Kleider J P, et al. Determination of band offsets in a-Si:H/c-Si heterojunctions from capacitance–voltage measurements: capabilities and limits. Thin Solid Films, 2007, 515(19): 7481
[5] De Wolf S, Kondo M. Abruptness of a-Si:H/c-Si interface revealed by carrier lifetime measurements. Appl Phys Lett, 2007, 90: 042111
[6] Stangl R, Kriegel M, Schmidt M. AFORS-HET, Version 2.2, A numerical computer program for simulation of heterojunction solar cells and measurements. Proceedings of the Fourth World Conference on Photovoltaic Energy Conversion, Hawaii, USA, 2006
[7] Powell M J, Deane S C. Defect-pool model and the hydrogen density of states in hydrogenated amorphous silicon. Phys Rev B, 1996, 53: 10121
[8] Eliott S R. Defect states in a-Si. Phil Mag B, 1978, 38: 325
[9] Shockley W, Read W T. Statistics of recombinations of holes and electrons. Phys Rev, 1952, 87: 835
[10] Hall R N. Electron–hole recombination in germanium. Phys Rev, 1952, 87: 387
[11] May G S, Sze S M. Fundamentals of semiconductor fabrication. Wiley John Wiley & Sons Inc, 2004
[12] Olibet S, Sauvain E V, Fesquet L, et al. Property of interfaces in amorphous/crystalline silicon heterojunctions. Phys Status Solidi A, 2010, 207: 1
[13] Aberle A G. Crystalline silicon solar cells advanced surface passivation and analysis. Center for Photovoltaic Engineering, University of New South Wales, Sydney, 1999
[14] Hoex B, Gielis J J H, van de Sanden M C M. On the c-Si surface passivation mechanism by the negative-charge-dielectric Al_2O_3. J Appl Phys, 2008, 104(11): 113703
[15] Glunz S W, Biro D, Rein S. Field-effect passivation of the SiO_2–Si interface. J Appl Phys, 1999, 86: 683
[16] Martin I, Vetter M, Garin M. Crystalline silicon surface passivation with amorphous SiC_x:H films deposited by plasma-enhanced chemical-vapor deposition. J Appl Phys, 2005, 98: 114912
[17] Anderson R L. Experiments on Ge–GaAs heterojunctions. Solid-State Electron, 1962, 5: 341
[18] Kleider J P, Gudovskikh A S, Cabarrocas P R. Determination of the conduction band offset between hydrogenated amorphous silicon and crystalline silicon from surface inversion layer conductance measurements. Appl Phys Lett, 2008, 92: 162101
[19] Van de Walle C G, Yang L H. Band discontinuities at heterojunctions between crystalline and amorphous silicon. J Vac Sci Technol B, 1995, 13: 1635
[20] Lequeux N, Cuniot M. Internal photoemission measurements on a-$Si_{1-x}Ge_x$:H/c-Si heterojunctions. J Non-Cryst Solids, 1989, 114(2): 555
[21] Hidenori M, Yoshinori H. Energy-band discontinuity in a heterojunction of amorphous silicon and crystalline Si measured by internal photoemission. Appl Phys Lett, 1987, 50: 326
[22] Ley L, Reichardt J, Johnson R L. Investigation of amorphous silicon with synchrotron radiation. Proc17th International Conference on Physics of Semiconductors, Springer-Verlag, New York, 1985: 811
[23] Jensen N, Rau U, Hausner R M, et al. Recombination mechanisms in amorphous silicon/crystalline silicon heterojunction solar cells. J Appl Phys, 2000, 87: 2639
[24] Zhao L, Zhou C L, Li H L, et al. Role of the work function of transparent conductive oxide on the performance of amorphous/crystalline silicon heterojunction solar cells studied by computer simulation. Phys Status Solidi A, 2008, 205(5): 1215
[25] Van de Walle C G, Martin R M. "Absolute" deformation potentials: formulation and *ab initio* calculations for semiconductors. Phys Rev Lett, 1989, 62: 2028
[26] Hamberg I, Granqvist C G. Evaporated Sn-doped In_2O_3 films: basic optical properties and applications to energy-efficient windows. J Appl Phys, 1986, 60: 123
[27] Jensen N, Hausner R M, Bergmann R B, et al. Optimization and characterization of amorphous/crystalline silicon heterojunction solar cells. Prog Photovoltaics, 2002, 10(1): 1
[28] Rahmouni M, Datta A, Chatterjee P, et al. Carrier transport and sensitivity issues in heterojunction with intrinsic thin layer solar cells on N-type crystalline silicon: a computer simulation study. J Appl Phys, 2010, 107(5): 054521
[29] Fujiwaraa H, Kondo M. Impact of epitaxial growth at the heterointerface of a-Si:H/c-Si solar cells. Appl Phys Lett, 2007, 90(1): 013503